Cite this: *Soft Matter*, 2011, **7**, 9167

www.rsc.org/softmatter

PAPER

Photoresponsive polymersomes as smart, triggerable nanocarriers†

Etienne Cabane, Violeta Malinova, Sindhu Menon, Cornelia G. Palivan and Wolfgang Meier*

Received 12th May 2011, Accepted 25th July 2011
DOI: 10.1039/c1sm05880k

The need for sophisticated systems to improve drug delivery to the body is growing, as is the complexity of therapeutic agents available to treat a variety of conditions. Among the requirements for intelligent drug delivery systems (DDS), responsiveness is highly desirable as a means to control pharmacokinetics and pharmacodynamics. Here, we study the potential of polymeric vesicles obtained from the self-assembly of a photocleavable amphiphilic block copolymer as a light-triggered DDS. The vesicles disintegrate upon UV irradiation, yielding small micellar-like structures, and simultaneously releasing their payload. The versatility of our system is tested both for low molecular weight molecules (fluorescein and ATTO655 dye), and for proteins (enhanced green fluorescent protein). By varying the UV intensity, the payload is released in a controlled manner, as established by fluorescence spectroscopy and fluorescence correlation spectroscopy. Therefore, these responsive polymer vesicles serve as smart, triggerable nanocarriers that can be applied to a variety of payloads, ranging from conventional drug molecules to proteins, enzymes, or DNA.

Introduction

Nowadays, conventional drug delivery systems (DDS), such as solid or liquid formulations for oral delivery and subcutaneous or intravenous injections, are the preferred routes of administration for a majority of active molecules. However, these systems are susceptible to various drawbacks, including lack of control over drug release and poor specificity when targeting cells or tissues. Therefore, the development of truly intelligent DDS should aim to improve therapeutic drug efficacy simply by allowing a molecule to find its target and to release at a predetermined rate and time.

The self-assembly of amphiphilic block copolymers with various architectures, including diblocks[1–4] and triblocks,[5–7] but also dendritic[8–10] and graft[11] copolymers, has been shown to form a variety of supramolecular structures.[12–14] Among these morphologies, polymer vesicles (also referred to as polymersomes) are currently under great scrutiny, due to their high potential to serve as drug delivery systems. Structurally, polymer vesicles are very similar to liposomes. They are hollow spheres with an aqueous core, encapsulating hydrophilic drugs or other biological compounds, and separated from the outside medium by a membrane that traps hydrophobic compounds. However, these synthetic structures outperform liposomes. They have elastic and robust membranes thicker and far more stable than liposomes' membranes.[1,15] In addition, recent advances in polymerization techniques have allowed the introduction of new functionalities and a variety of possible chemistries to amphiphilic block copolymers. In this respect, it is possible to introduce chemically active monomers or biologically active moieties that confer responsiveness to these polymersomes and the ability to reach a specific target. Tailoring the properties of polymersomes with respect to various stimuli, such as light, pH, or temperature, makes them suitable for medical applications, acting as "smart" systems.

The so-called stimuli-responsive polymers used in the fabrication of responsive superstructures undergo rapid changes in microstructure as a response to either external (ultrasounds, light) or internal stimuli (pH, temperature, oxidation, reduction). The response to these stimuli may be a modification of global hydrophilicity,[16–18] the selective degradation of one block,[19–21] or the cleavage of a linker.[22–24] Their common aim is destabilization of the membrane in order to induce either permeability due to poration,[25] or rupture followed by vesicle destruction.[18]

Light is a particularly attractive stimulus because it provides precise temporal (when the light source is switched on) and spatial (where the light is directed) control.[26,27] Furthermore, light-responsive systems do not require additional substances to trigger release and, as a result, do not modify the local polymersome environment. Several studies on light responsive systems have been reported, mainly including liposomes,[26,28–32] and micelles,[33–36] but only a few are dedicated to polymersomes.[37–41] Focusing on light-responsive polymersomes, it is worth noting that most of those groups proposed micron-size vesicles. It is well known that carrier size is a key feature in the design of an ideal drug delivery system, because it is linked directly to its blood clearance and circulation time.[17,42] To the

Department of Chemistry, University of Basel, Klingelbergstrasse 80, 4056 Basel, Switzerland. E-mail: wolfgang.meier@unibas.ch

† Electronic Supplementary Information (ESI) available: Additional experimental data. See DOI: 10.1039/c1sm05880k/

best of our knowledge, only one report of effective drug release from light-responsive vesicles of diameters below 300 nm has been published to date.[43] This motivated us to develop light-responsive polymersomes as efficient DDS.

We recently reported the synthesis of a new, photocleavable amphiphilic block copolymer, poly(methyl caprolactone)-*ONB*-poly(acrylic acid) (PMCL-*ONB*-PAA) that self-assembles into micelles and polymersomes (150 nm diameter).[22] The copolymer consists of the seldom used poly(methyl caprolactone), an amorphous hydrophobic, biocompatible and biodegradable polymer obtained *via* living ring opening polymerization (ROP),[44] and a water soluble and biodegradable poly(acrylic acid),[45] obtained *via* atom transfer radical polymerization (ATRP). Light-responsiveness was introduced by a photocleavable linker, O-nitrobenzyl (ONB), placed between the two polymer blocks. UV-irradiation induced a successful cleavage of the diblock copolymer chains, both in solvent (THF) and in aqueous solution, as well as of their self-assembled supramolecular structures (micelles and vesicles).

Here, we are interested in delving into greater detail regarding the UV-induced degradation mechanism of self-assembled superstructures of this copolymer, in order to understand how to optimize them in terms of a controlled release. To demonstrate their potential as DDS, we encapsulated and triggered the release of small hydrophilic molecules such as fluorescein and ATTO 655. Of greater interest was the encapsulation of proteins, such as enhanced green fluorescent protein (eGFP), inside the cavity of our light-responsive polymersomes, offering a new approach with potential in protein-based therapy. Irradiation conditions (time, dose) were varied and their effects on release kinetics were studied to optimize the system.

Experimental section

Materials

The synthesis of PMCL-*ONB*-PAA amphiphilic photocleavable block copolymers was described in a previous paper.[22]

Fluorescein (Aldrich), PBS (Dulbecco Aldrich), THF (inhibitor free, Aldrich), ATTO 655 (ATTO-TEC GmbH), enhanced green fluorescent protein in PBS buffer (EGFP, from Biovision) were used as received.

Preparation of self-assembled structures

Copolymer was dissolved in a minimum amount of inhibitor free THF to avoid UV light absorption by butylated hydroxytoluene (BHT). Then phosphate buffered saline (PBS) was added dropwise. The pH of the solution was adjusted to 7.4 with 0.5M NaOH solution (or HCl 0.5M). The solutions were allowed to equilibrate in the dark for three days, and then extruded through 1 μm, 0.4 μm and 0.2 μm filters to get rid of large size aggregates. Vesicles were isolated from micellar structures *via* size exclusion chromatography, SEC (Sepharose 2B, eluent PBS). We evaluated the final polymer concentration (*i.e.* after extrusion and SEC) using a fluorescence calibration curve. The fluorescence signal from the ONB linker was used for this calibration (Fig. S1, ESI†). Typical polymer concentrations range: 1 to 2 mg mL^{-1}. The solutions of empty vesicles were used to study the change in size and morphology of the self-assembled structures upon UV-irradiation.

Preparation of vesicles encapsulating small dye molecules and fluorescent protein

The different loads were encapsulated upon self-assembly of the copolymer using the co-solvent method.

Fluorescein. A solution of fluorescein in PBS buffer (25mM, quenching regime) was prepared, and added drop by drop to a polymer solution in THF. The mixture was allowed to equilibrate for three days in the dark, and then was extruded through 1 and 0.4 μm filters. Free fluorescein was removed by dialysis against fresh PBS buffer (for 2 mL of solution, 2 × 800 mL buffer exchange, then 800 mL overnight, using a 100 000 MWCO dialysis membrane), and SEC (Sepharose 2B, PBS).

ATTO655. Similar encapsulation procedure as above, using a 25 μM solution in PBS buffer. Extrusion with 1 and 0.4 μm filters prior to dialysis, but without performing SEC.

eGFP. Similar encapsulation procedure, with a 3 μM eGFP solution in PBS buffer. Extrusion with 1 and 0.4 μm filters prior to dialysis (with 300 000 MWCO membrane), but without performing SEC.

UV irradiation

Self-assembled AB2 polymer in PBS and loaded vesicle solutions were exposed to UV light provided by a Hamamatsu UV spot light source LC4 (200 W mercury-xenon lamp, spectral range 240 to 400 nm), equipped with a fiber optic light guide. The required irradiation wavelength (365 nm) was isolated using a set of UV filters (UG11 and WG 360, Schott Glass, see UV CO spectra in Fig. S2, ESI†). Samples were placed in quartz cuvettes, preferred to prevent UV absorption as from common glass vials. Several irradiation intensities were obtained as a function of light source to sample distance (Fig. S3, ESI†). Samples were irradiated using 20, 200, or 700 mW cm^{-2}, for a given amount of time. Experiments were conducted at room temperature (a temperature increase from 25 to 30 °C was observed with the highest energy used, but was considered insignificant for our applications).

Self-assembled structures size and morphology

Transmission Electron Microscopy (TEM) was employed as imaging technique to visualize the self-assembled copolymer structures (empty vesicles). 0.1 to 1.0 mg mL^{-1} solutions of polymer were placed on a copper grid (300 mesh), treated with glow discharge to make them hydrophilic. A drop of solution was placed on the grid, and the excess liquid was blotted. Then the grids were stained (2% uranyl acetate), followed by a rinsing step. TEM micrographs were acquired with a Philips Morgagni 268D instrument, operated at 80 kV.

The hydrodynamic radii and size distribution of the self-assembled copolymers (empty vesicles) were measured at room temperature by dynamic light scattering (scattering angle: 90°) with a commercial goniometer (ALV/CGS-8F, ALV Langen) equipped with a He:Ne linear polarized laser (JDS Uniphase,

wavelength = 632.8 nm). An ALV-5000/60X0 correlator was used to calculate the correlation function of the scattered light intensity, which was analyzed using the CONTIN algorithm. For static light scattering measurements, we used solutions with different polymer concentrations (from 0.1 to 1.0 mg mL^{-1}), at scattering angles from 40 to 150° with 10° angular steps. For each angle, three measurements of 100 s each were performed. For DLS and SLS data processing we used the ALV static & dynamic fit and plot software (version 4.31 10/01). SLS data were processed according to the Berry-model, and cumulant analysis.

Fluorescein release kinetics

The amount of released dye was followed at room temperature using fluorescence spectroscopy (on a Perkin Elmer, LS55). Irradiated samples of loaded vesicles were placed in quartz cuvettes and directly analyzed. The excitation wavelength was set at 494 nm and the emission spectra were recorded from 450 to 650 nm. The instrument was used in scan mode, with excitation slit set to 10 nm and emission slit set to 3 nm.

FCS

Fluorescence correlation spectroscopy (FCS) was performed with an inverted confocal fluorescence laser scanning microscope LSM 510 META/Confocor2 (Zeiss, Germany) equipped with an argon laser (for 405, 458, 477, 488 and 514 nm), and two helium-neon lasers (543 and 633 nm) as excitation sources. For FCS, 15 μL solution of loaded vesicles were applied to the glass surface of a cover glass (Huber & Co. AG, Switzerland) positioned on the xy-stage of the microscope. The excitation laser beam and the fluorescence emission passed through the same objective. The fluorescence signal was detected by highly sensitive avalanche photo diodes. Fluorescence intensity fluctuations were processed in terms of an autocorrelation function.

Results and discussion

Design of diblock copolymers and formation of polymersomes

The structure of the amphiphilic block copolymer is based on a photocleavable moiety (*O*-nitrobenzyl) acting as a junction between the hydrophilic poly(acrylic acid) (PAA) and hydrophobic poly(methyl caprolactone) (PMCL) blocks (Fig. 1). This molecule is efficiently cleaved upon irradiation with 365 nm UV light (as well as two-photon IR), concomitant with an intramolecular rearrangement.[46,47] We reported that, upon UV exposure, the diblock copolymer was rapidly split into two distinct polymer chains.[22] In addition, micellar (with a PMCL core and a PAA corona) and vesicular structures (the membrane of which is formed by interdigitated PMCL-PAA block copolymers) were obtained upon self- assembly of $PMCL_{105}$-*ONB*-PAA_{30} copolymer (AB1 in Table 1) in PBS buffer.[22]

Here, we self-assemble a $PMCL_{76}$-*ONB*-PAA_{16} diblock copolymer (AB2, in Table 1) under conditions similar to AB1. We changed the length of hydrophobic and hydrophilic blocks relative to AB1 in order to favor the formation of vesicles that were only a minor population in the case of AB1. The ability of AB2 to form vesicular structures was confirmed by dynamic and static light scattering (DLS and SLS) and transmission electron microscopy (TEM).

The size distribution histograms, obtained by DLS, indicate that the initial solution of self-assembled structures contains a major population with a hydrodynamic radius (R_h) of 80 nm. The major population and a secondary population with an R_h around 200 nm reveal the presence of large structures that could be either vesicles or micellar aggregates (Fig. 2). We calculated a ratio of 0.94 between the radius of gyration (R_g) and the hydrodynamic radius (R_h), using cumulant analysis and Berry plots (SLS data, Fig. S6, ESI†). This value is comparable to the theoretical value given for hollow spheres ($R_g/R_h = 1.0$),[48] and represents an indication that the two populations are vesicles. The presence of two vesicle populations indicates that structures obtained with AB2 are kinetically frozen structures. The second population (with R_h around 200 nm) may be removed by further extrusion through 0.1 μm filters.

TEM micrographs reveal the presence of spherical structures of diameters ranging from 100 to 150 nm, and only a few larger (diameter up to 500 nm, Fig. 2), which is in good agreement with the light scattering data. The combination of DLS, SLS, and TEM demonstrate that, when hydrated, $PMCL_{76}$-*ONB*-PAA_{16} block copolymers self-assemble into vesicles.

Degradation of polymersomes upon UV irradiation

Elucidating the UV degradation mechanism of vesicles is a key step in the investigation of their potential as smart, triggerable nanocarriers. The strategy of payload release from our system is based on exposing vesicles to UV light, inducing a subsequent degradation of the ONB linkers that cause the cleavage of

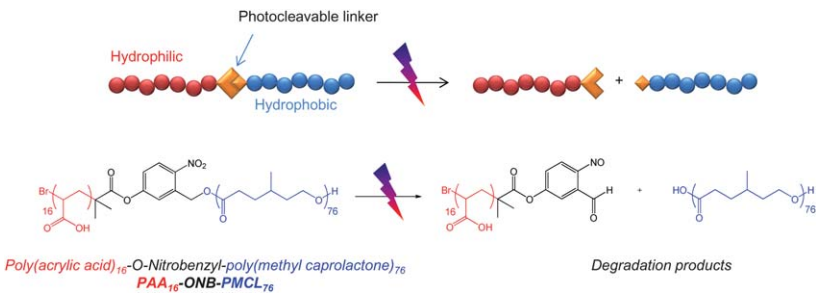

Fig. 1 Schematic view of the amphiphilic photocleavable block copolymer, chemical structure of the poly(methyl caprolactone)-*ONB*-poly(acrylic acid) diblock copolymer, and its degradation products upon UV irradiation. Upon cleavage, PAA chains bearing the photodegraded linker and PMCL chains bearing –COOH end groups are formed.

Table 1 Properties of AB diblock copolymers with different f ratios, used to form self-assemblies (NMR and GPC data for AB2 are given in the ESI†, Fig. S10 and S11)

Copolymer	DP (PMCL)[b]	DP (PAA)[b]	Mn (g mol^{-1})[b]	PDI[c]	f[d]
AB1[a]	105	30	17600	1.2	0.15
AB2	76	16	11300	1.2	0.11

[a] The AB1 copolymer was used in our previous study. [b] Degree of polymerization (DP) and number-average molecular weight (Mn) values calculated from ^{1}H-NMR. [c] Polydispersity index (PDI) obtained by GPC, using polystyrene standards. [d] Hydrophilic to hydrophobic mass ratio.

corona-forming PAA chains, and exposing the PMCL domains to water (Fig. 3). Because they are energetically unfavorable, these photodegraded supramolecular structures undergo a rearrangement at the macromolecular level to yield more favorable entities, or the hydrophobic domains simply precipitate The inner content of the vesicles is released during this transition (Fig. 3).

We observed the changes in size and morphology of the polymersomes caused by UV-irradiation in order to understand the responsiveness of the system and to propose a plausible degradation mechanism. The heat generated by UV-light exposure (temperature raised from 25 to 30 °C) was considered to have a negligible effect on vesicle stability. Number-averaged size distributions of a solution of vesicles measured after different irradiation times indicate that, during the irradiation process, vesicle size decreases (Fig. 4, full kinetics given in Fig. S4, ESI†).

After 20 min of irradiation with a dose of 200 mW cm^{-2}, both populations of initially observed intact vesicles (radii of 80 and 200 nm, Fig. 4A) were significantly reduced, and a distinct population of smaller entities appeared (Fig. 4B).

Conjecturably, those newly formed species, with a R_h of around 40 nm, are fragments of degraded vesicles. There were relatively few intact vesicles after 45 min of irradiation, and the major peak was associated with fragments of vesicles (Fig. 4C). In turn, these entities finally yield micellar-like structures, represented by the sharp peak with an R_h < 20 nm (Fig. 4D). Interestingly, even after 60 min of UV irradiation, a very small peak (accounting for 1% of the aggregates) can still be seen at 80 nm, indicating that a fraction of the vesicles is not destroyed (insert in Fig. 4D). A similar degradation sequence was observed when a lower UV irradiation dose (20 mW cm^{-2}) was applied to the same solution (Fig. S5, ESI†). In addition, a significant decrease in the mean count rate during the DLS experiment was observed (Fig. 5), as previously reported for photodegradable micelles,[36] and for redox sensitive micelles.[49] In general, the

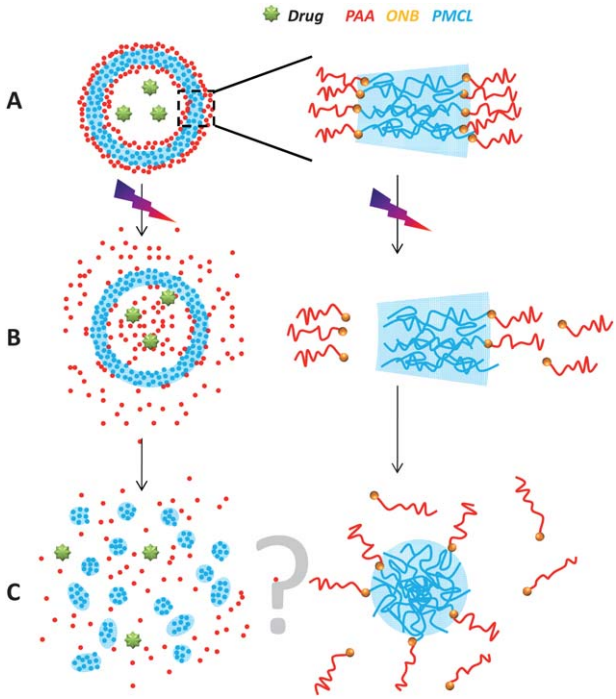

Fig. 3 Scheme depicting polymersomes, and the conformation of the assembled polymer chains forming their membranes (A). Upon UV exposure, the corona PAA chains are cleaved, *i.e.* separated from the PMCL, forming the core of the membrane (B). Consequently, the vesicle membrane is destroyed and the payload released (C).

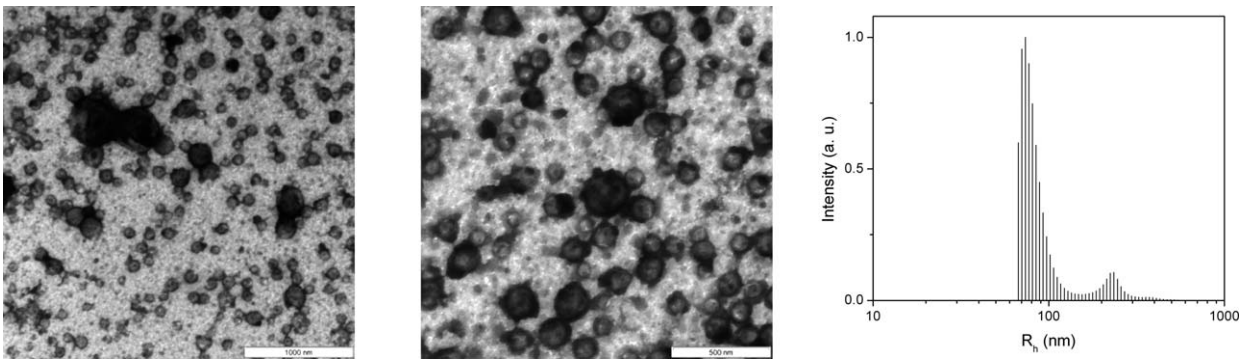

Fig. 2 Size distribution (from DLS), and TEM micrographs showing vesicles formed by self-assembly of $PMCL_{76}$-ONB-PAA_{16} in PBS, pH 7.4. Divergence in size of the objects observed by TEM and DLS is attributed to the difference in size between hydrated corona chains in water (DLS), and collapsed corona chains in the dry state (TEM). TEM scale bars: 1000 and 500 nm.

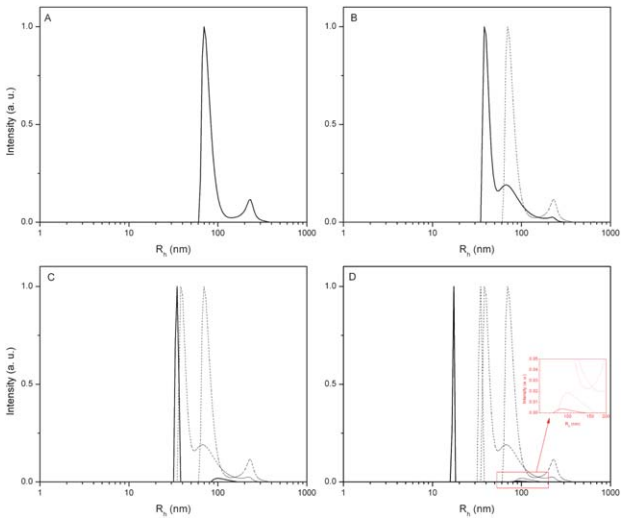

Fig. 4 Number-averaged size distributions obtained by dynamic light scattering (DLS). Three measurements at 90° for 300 s each were performed on samples irradiated (200 mW cm^{-2}) for different amounts of time. The correlation curves were fitted using the CONTIN method. (A) 0 min, (B) 20 min UV, (C) 45 min UV, and (D) 60 min UV.

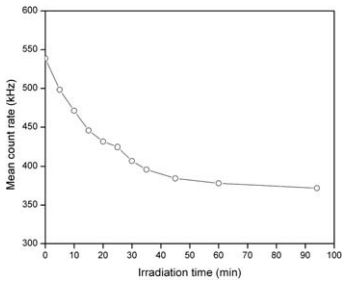

Fig. 5 Plot of mean count rate *vs.* irradiation time (200 mW cm^{-2}) for DLS experiment using AB2 vesicles in PBS. Values averaged over three measurements.

intensity decay is due to a lower number of aggregates in solution (correlated with the destruction of the initial particles and material precipitation), a decrease in their size, or a combination of both. Surprisingly, the UV exposure of the self-assembled PAA-*ONB*-PMCL chains is not accompanied by precipitation. This proves that, in this case, the observed decrease in mean count rate is solely associated with the disruption of vesicles to smaller particles.

We performed SLS on a vesicle solution after 94 min of UV irradiation to gain further insight into the morphology of the degraded structures, (Fig. S6, ESI†). The R_g/R_h ratio dropped from 0.94 for intact vesicles, to 0.88, a value that is higher than the typical ratio of 0.77, which is specific for micellar structures. The presence of still intact vesicles in solution is likely to explain this ratio.

We applied TEM to visually observe the morphology changes upon UV irradiation. The TEM micrographs show three different morphologies, corresponding to different stages of photodegradation: vesicles, broken vesicles, and finally micellar structures (Fig. 6).

The kinetics of vesicle degradation can be investigated by a change in size induced by UV irradiation over time (20 and 200 mW cm^{-2}, Fig. 7). When the lowest irradiation intensity was used, the decrease in size took place rather slowly. As expected, the process is faster when a higher intensity of UV is applied. This behavior correlates to the increased ONB degradation rate for higher UV intensities,[50] and can be used to tune the release rate of encapsulated compounds. The progressive change in size and morphology is correlated with the destruction of the initial vesicles and with the formation of micelles, as proposed in the summary included in Fig. 7.

UV-induced degradation mechanism of polymersomes

Although a triggered degradation mechanism of responsive polymersomes is not often discussed in detail, it is generally accepted that the destruction of vesicular structures is due to a loss of membrane integrity.[51] In the majority of stimuli-responsive vesicles, the membrane is destabilized *via* the alteration or modification of one of the polymer blocks. In the most common systems, hydrophobic segments are fractionated by acidolysis.[52] In this case, the stimulus causes a dramatic change in the hydrophilic/hydrophobic ratio (this ratio increases as the hydrophobic block is shortened),[53] and vesicles disintegrate to form micellar structures, a transition favored by this new hydrophilic/hydrophobic balance. In other systems, the hydrophilicity of a block can be tuned to obtain a fully hydrophilic copolymer chain, leading to dissolution of the membrane,[16,18,54,55] and causing the vesicle's destruction.

To our knowledge, the work of Katz and coworkers,[43] represents the only detailed example of a polymersome for which destabilization is induced by cleavage at the hydrophilic/hydrophobic interface. A diblock copolymer of poly(ethylene oxide) (PEO), which represents the hydrophilic part and with poly (caprolactone) (PCL) as the hydrophobic part and joined by a photocleavable moiety, self-assembled into vesicular structures. UV exposure induced a rearrangement of the cleaved PCL chains inside the membrane, resulting in a release of content. However, the vesicular structure was retained because the membrane was stabilized by the remaining, uncleaved PEO chains. After sufficient irradiation time, when all PEO chains were cleaved, the aggregates collapsed, and a precipitation occurred.

As the architecture of our diblock copolymer is similar, one would expect a comparable degradation mechanism. However, we observed completely different degradation behaviour after UV irradiation: no polymer precipitation occurs, and micellar structures are formed instead. These structures, consisting of purely hydrophobic blocks, are not conventional polymeric micelles (*i.e.* micelle formed by amphiphilic diblock copolymers), but rather "shaved micelles". The existence of such polymeric superstructures, due to electrostatic stabilization in water, was reported previously. In particular, aggregates such as unimolecular micelles[56] and dendrimers,[57] which have a hydrophobic core, can be electrostatically stabilized in aqueous solutions by functionalization with charged carboxylic head groups. Recently, Benaglia *et al.*[58] reported the formation of micelles composed of a completely hydrophobic block copolymer bearing a terminal carboxylic end group; the negatively charged corona

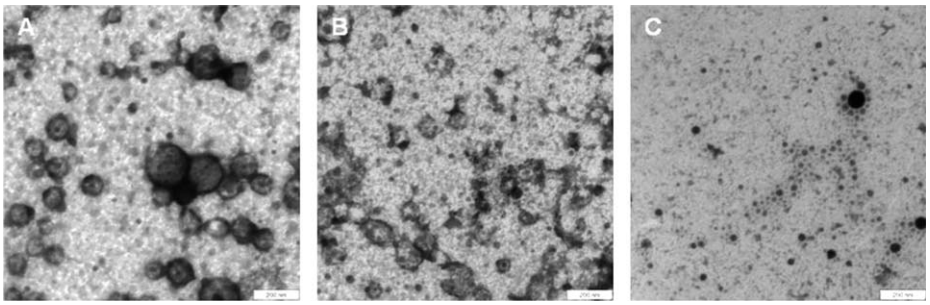

Fig. 6 Morphology change observed by TEM micrographs: (a) before UV, vesicles with diameters around 100 nm, (b) 25 min UV, broken vesicles and shapeless aggregates, and (c) 90 min UV, micelles and micellar aggregates. Scale bars are 200 nm. UV energy: 200 mW cm^{-2}.

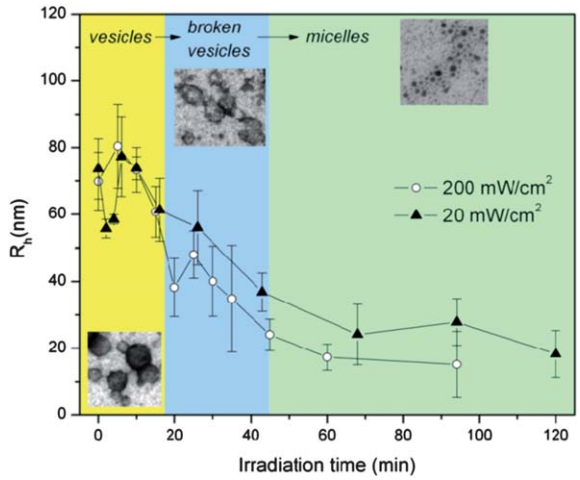

Fig. 7 Evolution of R_h *vs.* irradiation time, showing the transition from vesicles, to a mixture of broken vesicles and components of smaller size, and finally to micelles.

of the micelles stabilized the particles in an aqueous environment. In the case of our diblock copolymer AB2, the degradation pathway is based on the photolysis of the O-nitrobenzyl linker, generating a carboxylic end group on the cleaved poly(methyl caprolactone) chain (Fig. 1). These terminal weak acids ($pK_a \sim 4.5$) are negatively charged under the conditions that we use (*i.e.* PBS buffer, pH = 7.4).

Hence, there is a strong electrostatic repulsion in the outer part of the membrane (polymer-water interface) due to the ionic groups generated by cleavage of the ONB linker. A rearrangement takes place in the membrane in order to minimize this repulsion, occurring *via* an increase in the surface area available for negative charges. Because the area available for ionic head groups is proportional to $1/R$ (where R is the radius of the spherical particle),[59] the morphology will evolve from flat bilayer (extremely low curvature, high R value) to more favorable micellar structures (small R, high curvature). The supramolecular structures resulting from UV irradiation of AB2 vesicles are micelle-like particles formed by aggregated PMCL chains, stabilized by an ionic corona of charged carboxylic end groups (see Fig. 8). Additionally, uncleaved AB2 chains contribute to the stabilization of these aggregates in the early stage of the degradation process, explaining the transition structures observed by TEM and DLS. The size of the structures (approx. 20 nm in hydrodynamic radius) clearly indicates that they are formed by several PMCL chains. A putative scheme of the degradation mechanism is summarized in Fig. 8.

The different degradation behavior of our diblock copolymer compared to that reported by Katz *et.al.*[43] is due to the chemical nature of the photosensitive linker: O-nitrobenzyl linker yields a COOH residue upon cleavage, whereas the N-nitrobenzyl linker yields an amide residue.[60] As the amide is uncharged at physiological pH, there is no driving force toward the formation of micellar structures. In addition, poly(caprolactone), as a hydrophobic block,[43] is a crystalline polymer with reduced chain mobility, limiting a complete reorganization of the hydrophobic segments after cleavage.[13] In the case of PMCL, a totally amorphous homopolymer,[61] the flexibility of the chains is such that it provides fluidity to the membrane, which is able to adopt an alternate conformation and evolve toward a newly formed supramolecular structure.

Encapsulation and release of low molecular weight molecules

In order to test whether this system can be used as a photo-triggered nanocarrier, we studied the encapsulation of small hydrophilic molecules inside the aqueous cavity, and their release upon UV irradiation.

The loading of polymersomes with fluorescein and its release as a result of the exposure of polymersomes to UV was followed by fluorescence spectroscopy at different UV energies (Fig. 9). A significant increase in fluorescence intensity over time was obtained for the solutions of loaded vesicles exposed to UV, which was associated with the release of fluorescein (Fig. 9A–C). The solution of loaded vesicles that was kept in the dark showed no fluorescence increase over time, indicating that there was no leakage without UV irradiation (Fig. 9D).

In addition, release rates depended on the UV intensity: by increasing the UV intensity, a more rapid release was obtained (Fig. 9 and Fig. 10A). While 200 min were necessary to release about 40% of the encapsulated fluorescein by irradiation with an intensity of 20 mW cm^{-2}, only 20 min were necessary to release a similar fraction when an intensity of 700 mW cm^{-2} was used (Fig. 10B). The fact that the UV triggered release from AB2 vesicles is highly dependent on the intensity of the irradiation can serve to control the release process.

We used fluorescence correlation spectroscopy (FCS) to gain further insight into release behavior from AB2 polymersomes because it is a very sensitive method, detecting as little as a single

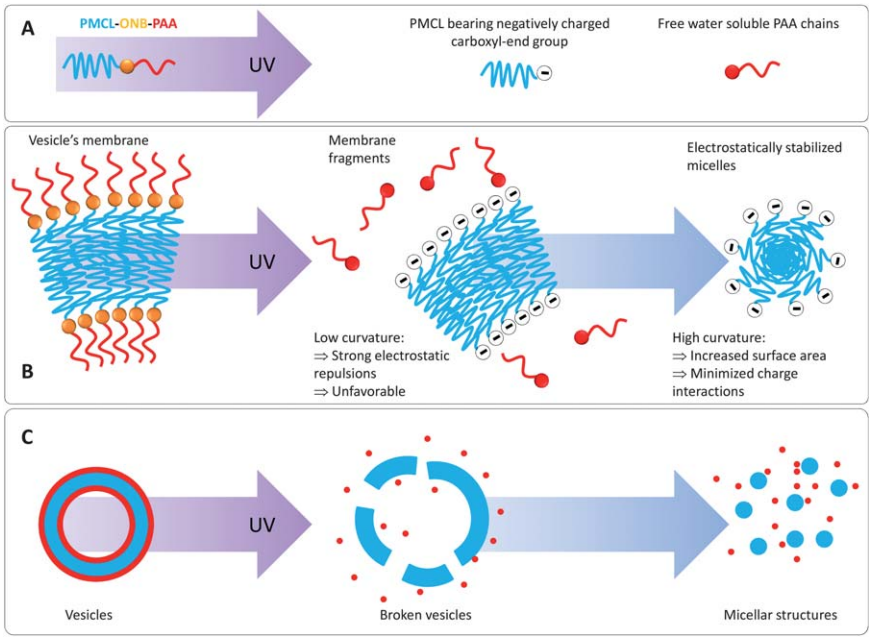

Fig. 8 Graphical summary depicting the proposed mechanism of polymersome degradation. (A) Molecular level: the diblock copolymer is rapidly cleaved upon UV irradiation; (B) supramolecular level: as a result of chain scission, packing of the PMCL chains forming the membrane is progressively destabilized and evolves into a more favourable arrangement; (C) aggregate morphology: from vesicles to broken vesicles to stabilized micellar structures.

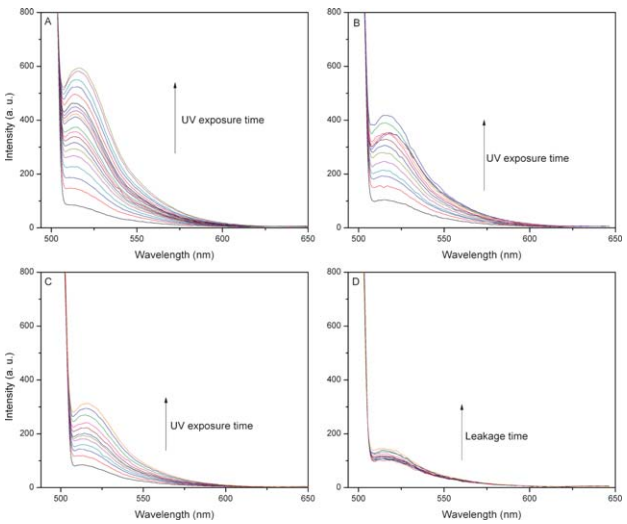

Fig. 9 Fluorescence spectra of fluorescein-loaded polymersomes exposed to different UV doses, showing the increase in fluorescence over time (from 0 to 311 min) due to release of the dye from a state of high concentration inside vesicles (self-quenching regime) to free dye in water (unquenched regime). (A) Irradiation with 700 mW cm^{-2}; (B) irradiation with 200 mW cm^{-2}; (C) irradiation with 20 mW cm^{-2}; (D) kept under dark conditions (*i.e.* no UV).

molecule. FCS provides diffusion time, number, and brightness of freely diffusing fluorescent molecules through a confocal volume of around 1 fL. The diffusion time can be used to determine the hydrodynamic radius of the particles by using the Stokes–Einstein equation.[62] We used FCS both to determine the amount of released dye from polymersomes as a function of irradiation time, and to calculate the size of the polymer superstructures present in solution. For encapsulation, we used ATTO655 dye instead of fluorescein, because it is more photostable while having a similar molecular weight (Fig. S7, ESI†).

We analyzed the autocorrelation curves using the least-squares fitting for two populations: free dye and polymersomes (Fig. 11, experimental curves given in Fig. S9, ESI†).[62] The average diffusion time (τ_D) of the free dye was 44 μs, while the τ_D for encapsulated dye inside polymersomes was 15.64 ms. Nearly 70% of dye was released after 15 min of UV irradiation, (Table 2). The fraction of free dye in solution increased with longer UV irradiation, and after 45 min ATTO655 was completely released (Fig. 11).

The diffusion times were used to estimate the R_h of loaded polymersomes and degraded supramolecular structures, respectively (see Table 2). Upon UV irradiation, the hydrodynamic radius of the supramolecular structures progressively decreased from 172 to 10 nm, in agreement with dynamic light scattering. Thus, UV irradiation triggers the disassembly of the polymersomes (R_h of 172 nm) to yield micellar structures (R_h of 10 nm).

Release of encapsulated eGFP upon UV irradiation

We investigated the encapsulation and release of enhanced green fluorescent protein using FCS, to prove the versatility of our smart UV-responsive polymersomes with respect to large molecules such as DNA and proteins. The encapsulation efficiency *e* defined as the ratio between the number of encapsulated eGFP molecules inside the inner volume of one vesicle and the theoretical maximal number of eGFP molecules fitting inside the same volume was estimated using the FCS data, and according to the calculations detailed in Supplementary Information. According to our calculations, we found an encapsulation

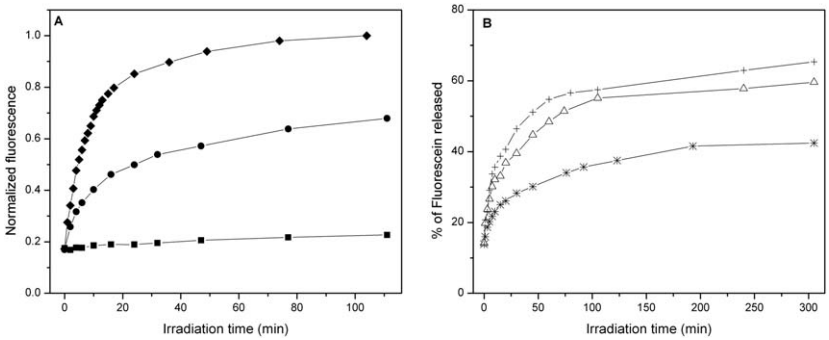

Fig. 10 (A) plot of normalized fluorescence (maximum emission intensity at $\lambda = 513$nm) *vs.* irradiation time for fluorescein-loaded polymersomes: (■) no irradiation, (●) irradiation with 20 mW cm^{-2}, and (◆) irradiation with 700 mW cm^{-2}. (B) percentage of Fluorescein released *vs.* irradiation time for fluorescein-loaded polymersomes exposed to different UV energies, showing energy dependent release kinetics: (*) 20 mW cm^{-2}, (△) 200 mW cm^{-2}, and (+) 700 mW cm^{-2}. Note: the percentage of dye released was estimated from comparison with the maximum fluorescence emission intensity obtained after mechanical destruction of the vesicles kept under dark conditions. The exact amount of released fluorescein is biased by the fraction of the dye that is affected by photobleaching. The release of fluorescein results in a fluorescence increase, while the photobleaching results in a fluorescence decrease, which amounts to a 20% loss of signal (at $\lambda_{max} = 513$nm, see Fig. S7, ESI†). The combination of those two opposing effects has been taken into account for the estimation of the released dye. It results in 78% released dye, but only 60% of it still being fluorescent (the rest is already photobleached).

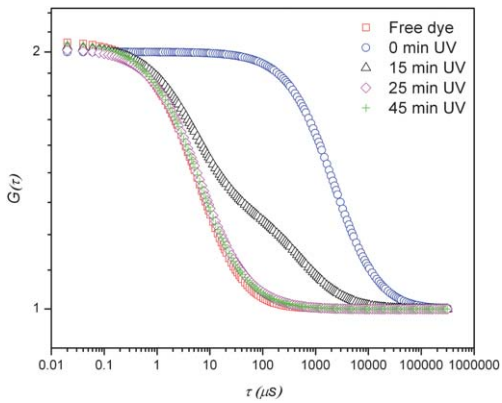

Fig. 11 FCS autocorrelation curves obtained for a solution of free ATTO655 in PBS (□), a solution of polymersomes loaded with ATTO655 under dark conditions (○), the same solution exposed to UV (15 min) (△), to 25 min UV (◇), and to 45 min UV (+). All curves were normalized to 2. UV energy: 200 mW cm^{-2}.

efficiency of 22%, which seems to be a reasonable estimation when compared to other systems of polymersomes encapsulating proteins.[63] During the release experiment, we expect that eGFP will not be affected by the slight temperature raise (25 to 30 °C) caused by the UV-irradiation.

The diffusion time of free eGFP was 98.5 μs, while it was 10.4 ms for the protein encapsulated in polymersomes (Table 3). The diffusion time of free proteins corresponds to a hydrodynamic radius of 2.2 nm, in good agreement with the reported radius of 2.3 nm.[64]

The solution of encapsulated eGFP kept in dark conditions did not indicate the presence of free protein (Table 3). After UV irradiation, the autocorrelation curve was fitted by taking into account the presence of two populations: free protein and encapsulated protein (labeled F_1 and F_2, respectively) (Fig. 12). That the fraction of free eGFP in solution (F_1) rapidly increased from 0 to 80% with UV exposure time indicates a gradual release of the protein in response to the UV trigger. The second fraction, which amounts to 17% (with a τ_D of 694 μs) corresponds to small structures, with a hydrodynamic radius of $R_{h,2} = 15$nm (see Table 3), and corresponds to released proteins that interact with free cleaved PAA chains.

In addition, the size of self-assembled structures dramatically changed upon UV irradiation. The fraction of eGFP released in solution correlates to the size decrease of the structures (Fig. 12). The change in the hydrodynamic radius upon UV exposure is in good agreement with the values obtained by dynamic light scattering, and supports the process of UV-mediated transition from vesicles to micelles, with a simultaneous release of the protein.

The release profiles of different payloads, ranging from low molecular weight compounds up to proteins, correlate with the time scale associated with the disassembly process of the vesicles. They indicate an immediate and modulated response (as a

Table 2 FCS results for vesicles encapsulating ATTO655 dye

Sample	F_1[%] [a]	$\tau_{D,1}$[μs][b]	$R_{h,1}$[nm][c]	F_2[%][a]	$\tau_{D,2}$[μs][b]	$R_{h,2}$[nm][c]
ATTO655, 52 nM in PBS	100	44	0.5	NA[d]	NA[d]	NA[d]
Loaded vesicles, UV = 0 min	0.01	44	0.5	99.9	15645	171.9
Loaded vesicles, UV = 15 min	70.1	44	0.5	29.9	5015	55.1
Loaded vesicles, UV = 25 min	96.4	44	0.5	3.6	1486	16.3
Loaded vesicles, UV = 45 min	97.9	44	0.5	2.1	950	10.4

[a] Fraction of component n. [b] Average diffusion time of fraction n. [c] Hydrodynamic radius of fraction n. [d] Not applicable.

Table 3 FCS evaluation of polymersomes loaded with eGFP

Sample	F_1[%][a]	$\tau_{D,1}$[μs][b]	$R_{h,1}$[nm][c]	F_2[%][a]	$\tau_{D,2}$[μs][b]	$R_{h,2}$[nm][c]
eGFP, 60 nM in PBS	100	98.5	2.2	NA[d]	NA[d]	NA[d]
Loaded vesicles, UV = 0 min	0	98.5	2.2	100	10384	231
Loaded vesicles, UV = 5 min	61	98.5	2.2	39	10096	224
Loaded vesicles, UV = 10 min	69	98.5	2.2	31	5691	126
Loaded vesicles, UV = 23 min	79	98.5	2.2	21	2439	54
Loaded vesicles, UV = 43 min	77	98.5	2.2	23	550	12
Loaded vesicles, UV = 60 min	83	98.5	2.2	17	694	15

[a] Fraction of component n. [b] Average diffusion time of fraction n. [c] Hydrodynamic radius of fraction n. [d] Not applicable.

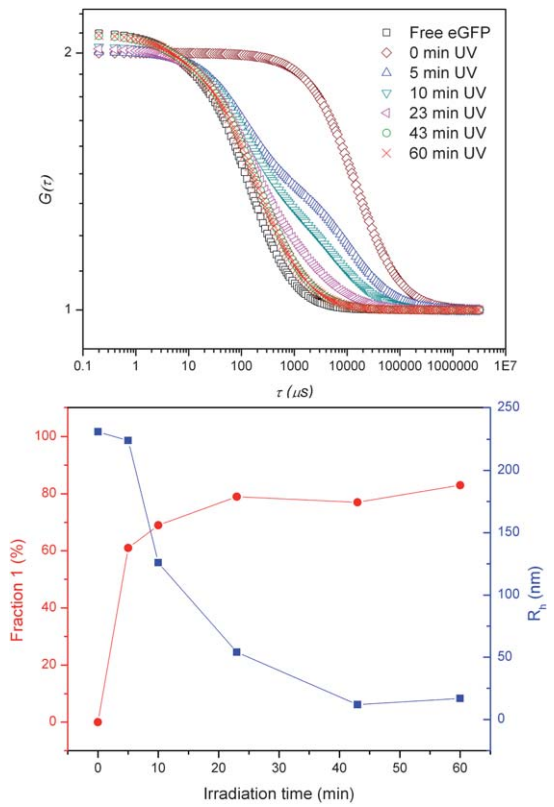

Fig. 12 Top: fitted FCS correlation curves of free eGFP and polymersomes loaded with eGFP irradiated for increasing amounts of time. Bottom: percentage of eGFP free in solution (fraction 1) as a function of irradiation time, and hydrodynamic radius (R_h) of supramolecular structures *vs.* irradiation time. All curves were normalized to 2. UV energy: 200 mW cm^{-2}.

function of UV intensity) of the polymersomes to the stimulus (UV light). When the light is switched on, both the transition from the vesicle to micelle and the release start simultaneously. This indicates that our system is sensitive enough to respond to the UV stimulus, even if a fraction of polymer chains remains uncleaved. Vesicle membranes are destabilized and rendered permeable to the encapsulated molecules in the very first minutes of irradiation.

If a slower degradation of vesicles is intended, mixing AB2 with a PMCL-PAA copolymer that is inert to UV irradiation should be considered. Indeed, blends of inert and hydrolysable copolymers that form vesicles have rates of release linearly dependent on the amount of degradable copolymer blended in the membrane, providing tunable release properties.[25] In our system, release rates can even be correlated to the number of photocleavable moieties, because PMCL-*ONB*-PAA copolymers comprise a single linker per chain.

Conclusions

We were interested in understanding how polymersomes that are formed by the self-assembly of a photocleavable amphiphilic block copolymer (PMCL-*ONB*-PAA) degrade upon UV-irradiation, and in demonstrating that they can be used as efficient photo-triggerable nanocarriers. We demonstrated the ability of vesicles to encapsulate payloads ranging from low molecular weight hydrophilic molecules (fluorescein and ATTO655) to proteins (eGFP), which supports the versatility of our system in various therapeutic applications. Polymer vesicles are disintegrated by UV irradiation within minutes, depending on the UV intensity. While the PAA-cleaved chains are solubilized in PBS, the cleaved hydrophobic chains are involved in the formation of new, supramolecular assemblies, coined as "shaved micelles". The payloads of the polymersomes are released upon reorganization of the polymer chains, *i.e.* membrane disintegration. As the release rates of the payload depend on UV intensity, the inner content of the photodegradable polymersomes can be released in a controlled manner, supporting the system as an efficient stimuli-responsive drug delivery system.

Acknowledgements

Financial support by the *Swiss National Science Foundation*, the *NCCR Nanosciences*, and the *Swiss Nanoinstitute* is gratefully acknowledged. EC thanks S. Egli and J. Braun, University of Basel, for interesting and useful discussions, and G. Persy for experimental assistance related to TEM. WM thanks in particular P. Vajkoczy. Authors thank M. Inglin, University of Basel, for manuscript editing.

Notes and references

1 H. Bermudez, A. K. Brannan, D. A. Hammer, F. S. Bates and D. E. Discher, *Macromolecules*, 2002, **35**, 8203–8208.
2 B. M. Discher, Y.-Y. Won, D. S. Ege, J. C. M. Lee, F. S. Bates, D. E. Discher and D. A. Hammer, *Science*, 1999, **284**, 1143–1146.
3 H. Kukula, H. Schlaad, M. Antonietti and S. Förster, *J. Am. Chem. Soc.*, 2002, **124**, 1658–1663.
4 L. Zhang and A. Eisenberg, *Science*, 1995, **268**, 1728–1731.
5 C. Nardin, T. Hirt, J. Leukel and W. Meier, *Langmuir*, 2000, **16**, 1035–1041.

6 A. Wittemann, T. Azzam and A. Eisenberg, *Langmuir*, 2007, **23**, 2224–2230.
7 W. Zhao, D. Chen, Y. Hu, G. M. Grason and T. P. Russell, *ACS Nano*, 2011, **5**, 486–492.
8 J. del Barrio, L. Oriol, C. Sánchez, J. L. Serrano, A. Di Cicco, P. Keller and M.-H. Li, *J. Am. Chem. Soc.*, 2010, **132**, 3762–3769.
9 Z. Shi, Y. Zhou and D. Yan, *Macromol. Rapid Commun.*, 2008, **29**, 412–418.
10 J. C. M. van Hest, D. A. P. Delnoye, M. W. P. L. Baars, M. H. P. van Genderen and E. W. Meijer, *Science*, 1995, **268**, 1592–1595.
11 H. J. Lee, S. R. Yang, E. J. An and J.-D. Kim, *Macromolecules*, 2006, **39**, 4938–4940.
12 A. Choucair and A. Eisenberg, *Eur. Phys. J. E*, 2003, **10**, 37–44.
13 R. C. Hayward and D. J. Pochan, *Macromolecules*, 2010, **43**, 3577–3584.
14 S. J. Holder and N. A. J. M. Sommerdijk, *Polym. Chem.*, 2011, **2**, 1018–1028.
15 O. Onaca, R. Enea, D. W. Hughes and W. Meier, *Macromol. Biosci.*, 2009, **9**, 129–139.
16 J. Du, Y. Tang, A. L. Lewis and S. P. Armes, *J. Am. Chem. Soc.*, 2005, **127**, 17982–17983.
17 A. Napoli, M. Valentini, N. Tirelli, M. Muller and J. A. Hubbell, *Nat. Mater.*, 2004, **3**, 183–189.
18 S. Qin, Y. Geng, D. E. Discher and S. Yang, *Adv. Mater.*, 2006, **18**, 2905–2909.
19 F. Ahmed, R. I. Pakunlu, A. Brannan, F. Bates, T. Minko and D. E. Discher, *J. Controlled Release*, 2006, **116**, 150–158.
20 P. P. Ghoroghchian, G. Li, D. H. Levine, K. P. Davis, F. S. Bates, D. A. Hammer and M. J. Therien, *Macromolecules*, 2006, **39**, 1673–1675.
21 F. Meng, C. Hiemstra, G. H. M. Engbers and J. Feijen, *Macromolecules*, 2003, **36**, 3004–3006.
22 E. Cabane, V. Malinova and W. Meier, *Macromol. Chem. Phys.*, 2010, **211**, 1847–1856.
23 S. Cerritelli, D. Velluto and J. A. Hubbell, *Biomacromolecules*, 2007, **8**, 1966–1972.
24 S. Lin, F. Du, Y. Wang, S. Ji, D. Liang, L. Yu and Z. Li, *Biomacromolecules*, 2007, **9**, 109–115.
25 F. Ahmed and D. E. Discher, *J. Controlled Release*, 2004, **96**, 37–53.
26 C. Alvarez-Lorenzo, L. Bromberg and A. Concheiro, *Photochem. Photobiol.*, 2009, **85**, 848–860.
27 F. Ercole, T. P. Davis and R. A. Evans, *Polym. Chem.*, 2010, **1**, 37–54.
28 R. H. Bisby, C. Mead and C. G. Morgan, *Biochem. Biophys. Res. Commun.*, 2000, **276**, 169–173.
29 R. H. Bisby, C. Mead and C. G. Morgan, *Photochem. Photobiol.*, 2000, **72**, 57–61.
30 B. Chandra, R. Subramaniam, S. Mallik and D. K. Srivastava, *Org. Biomol. Chem.*, 2006, **4**, 1730–1740.
31 T. S. Troutman, S. J. Leung and M. Romanowski, *Adv. Mater.*, 2009, **21**, 2334–2338.
32 S. Yagai, T. Karatsu and A. Kitamura, *Chem.–Eur. J.*, 2005, **11**, 4054–4063.
33 H.-i. Lee, W. Wu, J. K. Oh, L. Mueller, G. Sherwood, L. Peteanu, T. Kowalewski and K. Matyjaszewski, *Angew. Chem., Int. Ed.*, 2007, **46**, 2453–2457.
34 X. Liu and M. Jiang, *Angew. Chem., Int. Ed.*, 2006, **45**, 3846–3850.
35 Y. Zhao, *J. Mater. Chem.*, 2009, **19**, 4887–4895.
36 J. Jiang, X. Tong, D. Morris and Y. Zhao, *Macromolecules*, 2006, **39**, 4633–4640.
37 K. Han, W. Su, M. Zhong, Q. Yan, Y. Luo, Q. Zhang and Y. Li, *Macromol. Rapid Commun.*, 2008, **29**, 1866–1870.
38 Y. Jiang, Y. Wang, N. Ma, Z. Wang, M. Smet and X. Zhang, *Langmuir*, 2007, **23**, 4029–4034.
39 L. Lin, Z. Yan, J. Gu, Y. Zhang, Z. Feng and Y. Yu, *Macromol. Rapid Commun.*, 2009, **30**, 1089–1093.
40 E. Mabrouk, D. Cuvelier, F. o. Brochard-Wyart, P. Nassoy and M.-H. Li, *Proc. Natl. Acad. Sci. U. S. A.*, 2009, **106**, 7294–7298.
41 G. P. Robbins, M. Jimbo, J. Swift, M. J. Therien, D. A. Hammer and I. J. Dmochowski, *J. Am. Chem. Soc.*, 2009, **131**, 3872–3874.
42 F. Meng, Z. Zhong and J. Feijen, *Biomacromolecules*, 2009, **10**, 197–209.
43 J. S. Katz, S. Zhong, B. G. Ricart, D. J. Pochan, D. A. Hammer and J. A. Burdick, *J. Am. Chem. Soc.*, 2010, **132**, 3654–3655.
44 J. A. Zupancich, F. S. Bates and M. A. Hillmyer, *Macromolecules*, 2006, **39**, 4286–4288.
45 R. Larson, E. Bookland, R. Williams, K. Yocom, D. Saucy, M. Freeman and G. Swift, *Journal of Polymers and the Environment*, 1997, **5**, 41–48.
46 I. Aujard, C. Benbrahim, M. Gouget, O. Ruel, J.-B. Baudin, P. Neveu and L. Jullien, *Chem.–Eur. J.*, 2006, **12**, 6865–6879.
47 A. Blanc and C. G. Bochet, *J. Am. Chem. Soc.*, 2004, **126**, 7174–7175.
48 J. Hotz and W. Meier, *Langmuir*, 1998, **14**, 1031–1036.
49 Y. Kakizawa, A. Harada and K. Kataoka, *J. Am. Chem. Soc.*, 1999, **121**, 11247–11248.
50 D. R. Griffin, J. T. Patterson and A. M. Kasko, *Biotechnol. Bioeng.*, 2010, **107**, 1012–1019.
51 J. F. Le Meins, O. Sandre and S. Lecommandoux, *Eur. Phys. J. E*, 2011, **34**, 14.
52 D. E. Discher and F. Ahmed, *Annu. Rev. Biomed. Eng.*, 2006, **8**, 323–341.
53 D. A. Christian, S. Cai, D. M. Bowen, Y. Kim, J. D. Pajerowski and D. E. Discher, *Eur. J. Pharm. Biopharm.*, 2009, **71**, 463–474.
54 H. Lomas, I. Canton, S. MacNeil, J. Du, S. P. Armes, A. J. Ryan, A. L. Lewis and G. Battaglia, *Adv. Mater.*, 2007, **19**, 4238–4243.
55 A. Napoli, M. J. Boerakker, N. Tirelli, R. J. M. Nolte, N. A. J. M. Sommerdijk and J. A. Hubbell, *Langmuir*, 2004, **20**, 3487–3491.
56 W. Dong, Y. Zhou, D. Yan, H. Li and Y. Liu, *Phys. Chem. Chem. Phys.*, 2007, **9**, 1255–1262.
57 C. J. Hawker, K. L. Wooley and J. M. J. Frechet, *J. Chem. Soc., Perkin Trans. 1*, 1993, 1287–1297.
58 M. Benaglia, A. Alberti, E. Spisni, A. Papi, E. Treossi and V. Palermo, *J. Mater. Chem.*, 2011, **21**, 2555–2562.
59 S. Liu, T. Hu, H. Liang, M. Jiang and C. Wu, *Macromolecules*, 2000, **33**, 8640–8643.
60 P. H. N. Celie, M. Toebes, B. Rodenko, H. Ovaa, A. Perrakis and T. N. M. Schumacher, *J. Am. Chem. Soc.*, 2009, **131**, 12298–12304.
61 M. Trollsas, M. A. Kelly, H. Claesson, R. Siemens and J. L. Hedrick, *Macromolecules*, 1999, **32**, 4917–4924.
62 P. Rigler and W. Meier, *J. Am. Chem. Soc.*, 2005, **128**, 367–373.
63 O. Onaca, D. W. Hughes, V. Balasubramanian, M. Grzelakowski, W. Meier and C. G. Palivan, *Macromolecular Bioscience*, 2010, **10**, 531–538.
64 Z. k. Petráaek and P. Schwille, *Biophys. J.*, 2008, **94**, 1437–1448.

